# Improving the Clipping-based Active Constellation Extension PAPR Reduction Technique for FBMC Systems

Zahraa Tagelsir<sup>1,2</sup>, and Zsolt Kollár<sup>1</sup>

Abstract-Filter Bank MultiCarrier (FBMC) systems are known for their superior spectral efficiency and flexibility of the spectral shape. These benefits are challenged by the high Peak-to-Average Power Ratio (PAPR) and the Complementary Cumulative Distribution Function (CCDF) of the modulated signal, degrading power amplifier efficiency and system performance, causing spectral leakage and increasing Bit Error Rate (BER). This paper investigates the possibility of improvement for clipping-based Active Constellation Extension (ACE) based PAPR reduction techniques for FBMC systems. A modified method is proposed, combining iterative clipping and enlipping. A dynamic Clipping Ratio (CR) selection method is provided to optimize the iterative process. The method also enhances the BER performance by leveraging an enlipping step to increase the transmit signal power. Furthermore, the complexity of the iterative process is reduced by applying efficient and low computational FBMC modulation and demodulation schemes. The simulation outcomes validate that the suggested method efficiently reduces PAPR, optimizes the CCDF and improves the BER performance. Furthermore, the proposed system complexity is also reduced compared to the previous solutions.

Index Terms—FBMC, PAPR, clipping, enlipping, ACE, CR.

#### I. INTRODUCTION

RILTER Bank MultiCarrier modulation using Offset Quadratic Amplitude Modulation (FBMC-OQAM) system is a multicarrier modulation technology that is a promising physical layer candidate for 5G and 6G communication networks. The central concept of FBMC is to boost the time duration of the symbols in the time domain using a prototype filter. The symbols are designed so that they overlap both in time- and frequency-domain. The overlap in the time domain makes it possible to maintain the original data transmission rate, and the frequency-domain overlap results in a welllocalized spectral shape [1].

An inherent challenge in MultiCarrier (MC) transmission schemes like FBMC is the elevated Peak-to-Average Power Ratio (PAPR). This issue arises due to the unique structure of the MC signal, in which numerous independently modulated subcarriers are transmitted in parallel. In certain conditions, the phases of the subcarriers may align constructively, resulting in signal peaks that are significantly higher than the average signal power. While the probability of such extreme peaks is

Department of Artificial Intelligence and Systems Engineering, Faculty of Electrical Engineering and Informatics, Budapest University of Technology and Economics, Budapest, Hungary.

E-mail: {zahraa, kollarzs}@mit.bme.hu

Department of Electrical and Electronic Engineering, Faculty of Engineering, Red Sea University, Port Sudan, Sudan.

DOI: 10.36244/ICJ.2025.3.6

relatively low, in practice, such signals exhibit considerably higher PAPR values than their single-carrier counterparts [2].

Power Amplifiers (PAs) are designed to operate efficiently near their saturation point, but high PAPR forces them into nonlinear regions, causing significant distortions; the nonlinear effects include spectral spreading, intermodulation, and warping of signal constellations, which degrade system performance. A large input back-off is also required to prevent the PA from operating in its nonlinear region, reducing the amplifier's power efficiency [3]. The nonlinearities result in in-band distortion; the amplified signal experiences different gains, which degrades Bit-Error Rate (BER) performance by introducing additive noise and out-of-band distortion, where intermodulation generates undesired frequency components at frequencies outside the signal range, which leads to interference with adjacent channels [2].

Various studies have explored different aspects of FBMC, including its implementation challenges and optimization techniques. In [4], a lower bound on the achievable PAPR reduction using optimization-based approaches is established.

Numerous schemes have been introduced to reduce PAPR in FBMC systems. These include coding [5], Partial Transmit Sequence (PTS) [6], Companding techniques [7], Selected Mapping (SM) [8], Tone Injection (TI) [9], Tone Reservation (TR) [10] or Active constellation extension [11]. However, while these methods aim to reduce the high PAPR, they have drawbacks, such as:

- increased computational complexity,
- reduced data rate,
- required side information for demodulation,
- increased bit error rate.

This paper investigates the optimization possibilities for the ACE-based PAPR reduction technique for FBMC modulation, as this technique does not reduce the data rate nor require any side information for the demodulation process. The only drawback of this technique is that soft demodulation in the receiver is not possible, as the constellation points are predistorted. Thus, the decoding gain for complex channel coding such as Turbo codes, Low-Density Parity Check (LDPC) or Polar codes is lost [12]. Furthermore, ACE can be jointly used effectively with an iterative clipping and filtering-based technique, as presented in [11].

An adaptive Clipping Ratio (CR) optimization approach is proposed, where the CR values are dynamically tuned across multiple iterations to effectively minimize the PAPR of the signal. Furthermore, a novel hybrid method is introduced, combining clipping and enlipping [13]. This approach combines the advantages of both techniques and improves BER performance by amplifying the signal power in the last enlipping process. Furthermore, a signal processing complexity reduction of the iterative modulation-demodulation of the FBMC signal is also proposed to enable a practical implementation.

The proposed method enhances the gain metric, which balances PAPR reduction and the additional signal power by significantly reducing PAPR with fewer iterations than conventional methods. Moreover, the proposed scheme shows an improvement in complexity by requiring fewer iterations for a comparable or better performance, which reduces the computational overhead of iterative PAPR reduction techniques. Therefore, it enhances the proposed technique's effectiveness regarding performance and is more computationally efficient, addressing a critical trade-off in communication system design.

The primary contributions of this paper are:

- An optimized CR selection strategy across iterations is provided.
- A modified PAPR reduction technique using ACE is proposed, combining iterative clipping and enlipping.
- A reduced computational complexity of the iterative structure is also proposed that requires fewer signal processing steps.

The paper is structured as follows. In the next section, the FBMC system model is introduced, and a statistical analysis of the signal is given, including an evaluation of the Complementary Cumulative Distribution Function (CCDF) of PAPR and the kurtosis for various numbers of subcarriers. The ACE-based PAPR reduction technique, which uses iterative clipping and filtering, is discussed in Section III. Section IV introduces the proposed improvements; the results are verified using simulations. Section V discusses complexity reduction possibilities of the iterative process, and analytical derivations are given for the required number of multiplications. Section VI concludes the paper with key findings and contributions.

## II. FBMC MODULATION

FBMC is a multicarrier modulation technique with high potential for the physical layer of future communication systems. In this scheme, the binary data is first converted into complex symbols through Quadrature Amplitude Modulation (QAM). The resulting symbols are then split into real and imaginary parts, each undergoing a phase rotation and passing through a prototype filter. To maintain orthogonality, the real and imaginary parts are transmitted with a half-symbol time offset (OQAM). After filtering, the components are modulated to different subcarriers, and the combined terms form the final baseband output signal [14]. The resulting FBMC-OQAM signal can be mathematically described as follows:

$$x[n] = \sum_{m=-\infty}^{\infty} \sum_{k=0}^{N-1} \left( \theta^k \Re(X_k[m]) f_0[n - mN] + \theta^{k+1} \Im(X_k[m]) f_0[n - mN - N/2] \right) e^{j\frac{2\pi}{N}kn}. (1)$$

where:

- X<sub>k</sub>[m]: The complex QAM symbol mapped to subcarrier k at time instant m.
- $\Re(X_k[m])$ ,  $\Im(X_k[m])$ : The real and imaginary parts of the complex symbol  $X_k[m]$ ,
- $\theta^k$  and  $\theta^{k+1}$ : Phase rotation terms:  $\theta = e^{j\frac{\pi}{2}}$ .
- $f_0[n-mN]$ : impulse response of the prototype filter,
- e<sup>j 2π/kn</sup>: the complex exponential term responsible for modulating the signal to the k<sup>th</sup> subcarrier.

One of the significant issues of FBMC systems is the high computational complexity, primarily resulting from the necessity of large-size IFFTs, especially when using the Frequency Spreading (FS) approach to implement the signal modulation/demodulation [1]. The PolyPhase Network (PPN) based transceiver structure eases this problem using polyphase filterbanks with smaller IFFTs [1]. One of the most efficient variants of the PPN-based transmitter is the modified PPN structure presented in [15], which employs a single IFFT combined with two PPN filters and some signal processing blocks. This structure is shown in Fig. 1. The structure significantly reduces the computational complexity compared to traditional implementations. In conventional PPN transmitters, two separate N-point IFFTs are required to process the real and imaginary parts of the signal independently. However, the modified PPN structure leverages a single IFFT to process both components simultaneously. Using a single IFFT block in the PPN structure effectively halves the number of complex multiplications required in the transmitter, making it a computationally efficient solution. This transmitter structure is used in this paper.

Similarly, Fig. 2 illustrates the corresponding PPN-FBMC receiver employing a single FFT. Traditional PPN-based receivers utilize two parallel FFT blocks to process the received signal's real and imaginary components independently. The enhanced PPN architecture substitutes these two FFTs with a single full-size FFT and some additional signal processing. The PPN filtering is initially applied, followed by correcting for the phase rotation factor from the transmitter using a circular shift in the opposite direction [15]. The overlapping real and imaginary segments of the FBMC-OQAM symbols are divided into even and odd components: the even component is derived from the real signal. In contrast, the odd components are received from the imaginary signal. These components are merged later to create complex time-domain symbols, which are subsequently processed by a single FFT to retrieve the transmitted QAM symbols [16]. This receiver structure will be used in this paper.

The statistical properties should also be investigated, as the FBMC signal can be considered multicarrier. The significant dynamic range of the FBMC signal presents a challenge as the signal at the transmitter goes through a PA, which may cause nonlinearities or operate inefficiently if not driven using the entire linear range. Applicable PAs do not preserve linearity across the entire signal dynamic range, leading to uneven amplification of various signal sections. This distortion affects the quality of the signal, resulting in a reduced BER performance [2].

Fig. 1: FBMC transmitter using a single IFFT block.

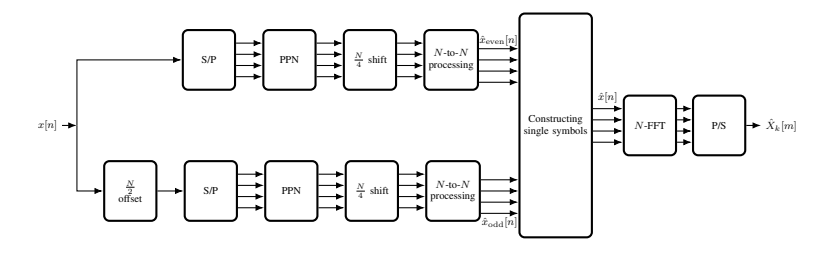


Fig. 2: FBMC receiver using a single FFT block.

To analyze the behaviour of the FBMC signals in the presence of such PAs and to investigate possible PAPR reduction techniques, the statistical metrics such as kurtosis and CCDF of the PAPR are examined for different numbers of subcarriers.

The kurtosis of these components for different subcarriers is evaluated to determine the similarity of the real and imaginary components of the FBMC signal to Gaussian characteristics as the number of subcarriers increases. The kurtosis is a statistical indicator of how often outliers appear. It provides a statistical description of a distribution's shape and relationship to the normal distribution [11]. The kurtosis  $\beta$  of the random variable  $\zeta$  is defined as:

$$\beta = \frac{\mathbb{E}[\zeta^4]}{\left(\mathbb{E}[\zeta^2]\right)^2}.$$
 (2)

It is the ratio of the variable's fourth moment to the square of its average power. A univariate normal distribution has a kurtosis of 3.

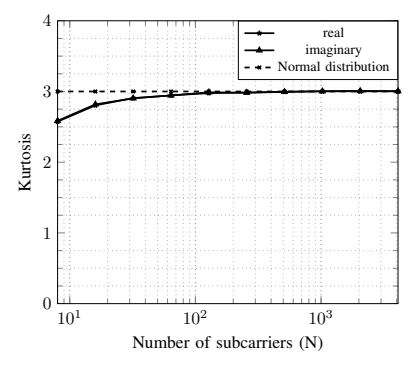


Fig. 3: Kurtosis of the real and imaginary part of the complex FBMC signal in function of the number of subcarriers.

The kurtosis of the real and imaginary parts of the complex baseband FBMC signal in function of the subcarriers can be seen in Fig. 3. As the number of subcarriers grows, the kurtosis values approach 3, indicating convergence toward a normal distribution. Above N=256 subcarriers, it can be concluded that the real and imagery parts of the FBMC signal are Gaussian distributed.

A further metric of the FBMC signal is the PAPR, which measures the difference between a signal's peak and average power. It can be used to characterize the study of the dynamic features of FBMC signals. The PAPR for the  $m^{\rm th}$  FBMC symbol can be expressed as:

$$PAPR(x_m[n]) = \frac{\max_{n \in [0, L-1]} (|x_m[n]|^2)}{E(|x_m[n]|^2)}.$$
 (3)

where L is the length of the prototype filter. Furthermore, the CCDF is used for the statistical distribution of the PAPR. The CCDF denotes the likelihood of the PAPR values surpassing a specified limit PAPR<sub>0</sub>:

$$CCDF = Prob(PAPR > PAPR_0).$$
 (4)

For the FBMC signal, the CCDF of the PAPR was analyzed for a different number of subcarriers. The CCDF can be seen in Fig. 4. It can be seen that a rising number of subcarriers leads to an increased PAPR due to the signal approaching a Gaussian distribution with a higher number of independent variables, consistent with the central limit theorem. This metric will also be used to assess the efficacy of the clipping-based PAPR reduction method presented in the next section.

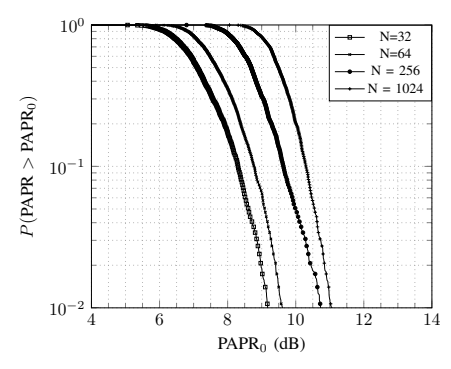


Fig. 4: CCDF of the PAPR of the FBMC symbols for different numbers of subcarriers.

# III. CLIPPING-BASED ITERATIVE PAPR REDUCTION VIA ${\bf ACE}$

This section briefly introduces the clipping-based PAPR reduction combined with ACE and filtering. This method was introduced and evaluated in [11].

#### A. Iterative clipping and filtering

Clipping is a non-linear signal processing technique that lowers the amplitude of peaks in a transmitted signal that exceeds a pre-defined threshold. It is done to minimize the signal's dynamic range and thus make it easier to transmit. The process entails clipping such high peaks while trying, as much as possible, to preserve the integrity of the underlying data. The clipped FBMC signal can be expressed as

$$x_{c}[n] = \begin{cases} x[n] & \text{if } |x[n]| \le A_{\text{max}} \\ A_{\text{max}} e^{j\phi(x_{n})} & \text{if } |x[n]| > A_{\text{max}} \end{cases}, \tag{5}$$

where  $x_{\rm c}[n]$  is the clipped signal, and  $A_{\rm max}$  is the clipping threshold. The clipping threshold is determined by a parameter called the CR, which is mathematically defined as:

$$CR_{dB} = 20 \log_{10}(\gamma) \tag{6}$$

with

$$\gamma = \frac{A_{\text{max}}}{\sqrt{P_r}},$$

where  $P_x$  is the signal power.

Clipping is simple to implement and computationally efficient, so it's an attractive choice for PAPR reduction. It can considerably increase the efficiency of power amplifiers by properly selecting the threshold value. However, clipping causes both in-band and out-of-band distortions, increasing BER and introducing unwanted distortion in the spectral shape. It can eliminate the out-of-band radiation after demodulating the signal and resetting the unused subcarriers to zero, i.e. filtering them out. Still, it will also increase the peaks of the newly generated signal. The in-band distortion can be handled in several ways; in the case of TR, some carriers are kept so that they are used for PAPR reduction purposes; in the case of ACE, the constellation points are allowed to be distorted as long as the no BER degradation is introduced during demodulation. This repeated interactive method using clipping and filtering with TR and ACE can be used effectively to reduce the PAPR of the FBMC signal. In the next subsection, the ACE method will be described in more detail.

# B. Active constellation extension

The concept of ACE was initially introduced in [17] for mitigating the PAPR in OFDM systems that employ QAM constellations. ACE is usually applied along with clipping to minimize the distortions introduced to the data subcarriers. ACE modifies the amplitude and phase of some of the constellation values located at the outer points of the constellation of the signal. These points can be shifted outwards, within permitted regions, to create a new representation of the same symbols. By using ACE on the subcarriers distorted by clipping, the QAM values are restored, and in parallel,

the BER performance is also improved while maintaining the clipped and distorted values of the given subcarrier for PAPR reduction.

A 4-QAM modulation is employed to optimize the constellation-shaping process, where four possible constellation points are evenly distributed across each quadrant of the complex plane, and constellation points are modified within the quarter-plane outside the nominal point. The extension regions for 2-QAM, 4-QAM and 16-QAM are depicted in Fig. 5. For higher-order modulations, the ACE is less effective as fewer QAM values can be extended toward outer regions, thus leading to a smaller improvement in the PAPR reduction performance of the time domain signal. During our investigations, we will use the constellation with 4-QAM.

# IV. IMPROVEMENTS TO THE CLIPPING BASED ACE $$\operatorname{\textsc{Method}}$$

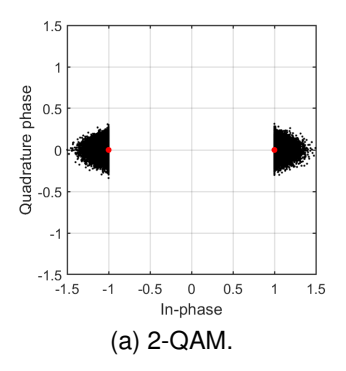
### A. Improving the clipping-based PAPR reduction scheme

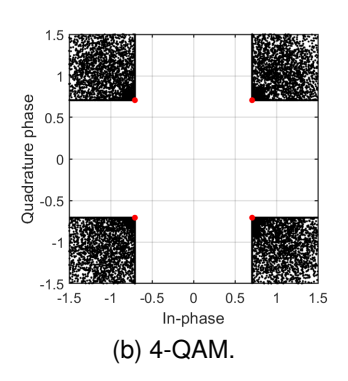
- 1) Fixed CR: The most straightforward approach involves maintaining the CR constant over the iterations. To evaluate the performance, the CCDF of the PAPR is observed at a specific probability after each iteration. The best CR value that achieves the smallest PAPR for a given number of iterations will be selected.
- 2) Adaptive CR: PAPR reduction techniques and iterative methods such as clipping combined with ACE are commonly used to achieve substantial reduction. However, traditional approaches often rely on a fixed CR across all iterations. While effective to an extent, this static approach does not leverage the evolving characteristics of the signal throughout the iterative process. An adaptive CR approach is also suggested in this paper to optimize the clipping thresholds across iterations dynamically. The algorithm optimizes the PAPR reduction process by systematically evaluating all possible combinations of CR values across iterations and selecting the sequence that achieves the minimum PAPR. This exhaustive search ensures the best possible PAPR reduction with controlled signal distortion. Similar to the fixed CR case, the CCDF of the PAPR is observed during the iterative process. During each iteration, the PAPR Reduction algorithm is implemented for different CRs. Once the set number of iterations has been completed, the CR values that achieve the most significant PAPR reduction are selected. The exhaustive search minimizes the PAPR by considering all possible combinations. This ensures better performance than fixed CR approaches.

#### B. Applying the enlipping technique

The suggested technique presents an innovative way to reduce iterative PAPR in FBMC systems. It combines conventional iterations of clipping and ACE with a final enlipping and ACE step. This method is designed to achieve superior PAPR reduction, minimize signal distortion, and improve BER performance. Enlipping, introduced in [13], involves adjusting the amplitude of each signal to its peak value instead of limiting the high peaks to a predetermined level:

$$x_{\mathbf{e}}[n] = A_{\max} e^{j\phi(x_n)},\tag{7}$$





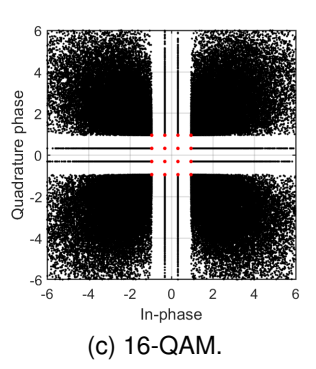


Fig. 5: Extension regions of ACE for 2-QAM, 4-QAM and 16-QAM. Red dots mark the ideal cancellation points.

where  $x_{\rm e}[n]$  is the enlipped signal,  $A_{\rm max}$  is the clipping threshold, and  $\phi$  is the signal phase. Despite the signal samples exceeding or falling below the clipping threshold  $A_{\rm max}$ , every signal sample will be modified to align with  $A_{\rm max}$  while preserving its phase value.

The unique feature of this method is found in the adaptive CR used in the clipping iterations and the enlipping process at the end. While clipping reduces the signal peaks to control PAPR, the final enlipping step increases the signal power without increasing the signal peaks, thereby improving BER by improving the SNR. This dual-action methodology navigates the compromise between PAPR minimization and overall system performance.

Clipping limits the signal peaks that exceed a given CR value, effectively reducing PAPR. However, this can distort the signal and cause constellation points to migrate outside their valid decision regions. When this happens, the receiver may misinterpret these points, resulting in significant BER degradation. ACE selectively moves the distorted points back to their legitimate constellation boundaries to solve this problem. The restoration process will ensure the modified symbols stay within acceptable decision regions to maintain the transmitted signal's integrity and ensure minimal BER degradation while maintaining effective PAPR reduction. The iterative method dynamically lowers PAPR, preparing it for the concluding stage. In the final step, we apply enlipping, then ACE, enlipping modifies all signal amplitudes to match a specified CR value, enhancing the average signal power. This stage offsets the losses caused by clipping in previous iterations.

The block diagram of the proposed modified iterative technique extended with enlipping is displayed in Fig. 6.

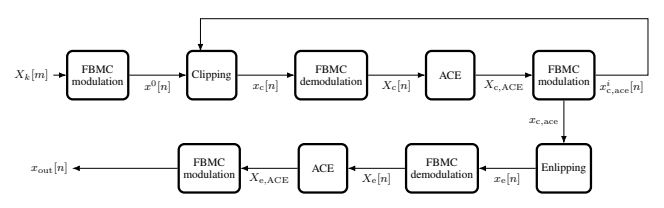


Fig. 6: Block diagram of the proposed iterative PAPR reduction scheme using ACE extended with enlipping for FBMC.

#### C. Simulation results

The parameters used throughout the simulation are outlined in Table I for the applied FBMC system. From the available 256 subcarriers, 170 were modulated, and an oversampling factor of 4 was applied to ensure that the peaks in the signal were well approximated. A 4-QAM is selected for the modulation alphabet so that the ACE can be well utilized while maintaining a relatively high data rate. During the simulation, the PHYDYAS filter is applied to the prototype filter with an overlapping factor (K) of 4. To have a statically large enough dataset for evaluating the PAPR, 1000 FBMC symbols were applied.

TABLE I SIMULATION PARAMETERS.

| Parameter                  | Value   |  |  |
|----------------------------|---------|--|--|
| Number of subcarriers (N)  | 256     |  |  |
| Number of data subcarriers | 170     |  |  |
| Modulation                 | 4QAM    |  |  |
| Oversampling               | 4       |  |  |
| Prototype filter           | PHYDYAS |  |  |
| Overlapping factor $(K)$   | 4       |  |  |
| Number of symbols          | 1000    |  |  |

The choice of the CR value over the iterations significantly influences the overall performance of PAPR reduction. The first step in the case of fixed CR is to identify which CR values result in the maximum PAPR reduction of the FBMC signal [18]. CR values ranging from (CR =  $0\,\mathrm{dB}$  to  $8\,\mathrm{dB}$ ) with steps of 0.25 dB were tested for 1,2 and 3 iterations to evaluate the effectiveness of the iterative method in reducing PAPR. The results are shown for different numbers of iterations in Fig. 7. The identified optimal CR values for different iterations are as follows:

- 5.25 dB achieving 9.92 dB PAPR value for 1 iteration,
- 5.25 dB achieving 9.26 dB PAPR value for 2 iterations,
- 5.50 dB achieving 8.81 dB PAPR value for 3 iterations.

Further optimization can be done using adaptive CR. Fig. 8 shows the obtained CR values for 3 iterations for different combinations throughout the iterative process. The results show that the best combination of CR values (CR<sub>1</sub> =  $4.50\,\mathrm{dB}$ , CR<sub>2</sub> =  $5.50\,\mathrm{dB}$ , CR<sub>3</sub> =  $5.75\,\mathrm{dB}$ ) was identified by exhaustively searching all possible combinations. The iteration process is also analyzed in details shown in Fig. 9. The

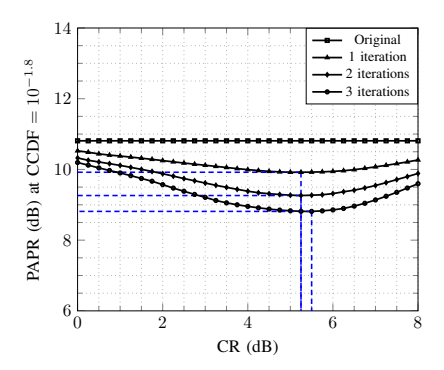


Fig. 7: Resulting PAPR with fixed CR over the iterations. Optimal CR values are indicated by dashed guides.

initial PAPR values are depicted with a dashed line, and a closely linear PAPR improvement throughout the iterations is shown in a solid line. Furthermore, the CR values used in the adaptive clipping with blue color show a slight logarithmic increase through the iterative process achieving a minimum PAPR of 8.79 dB in the target probability, resulting in a slight improvement of 0.02 dB compared to the fixed CR method. The gain can be increased by utilizing higher iteration counts; however, the computation complexity increases exponentially in parallel.

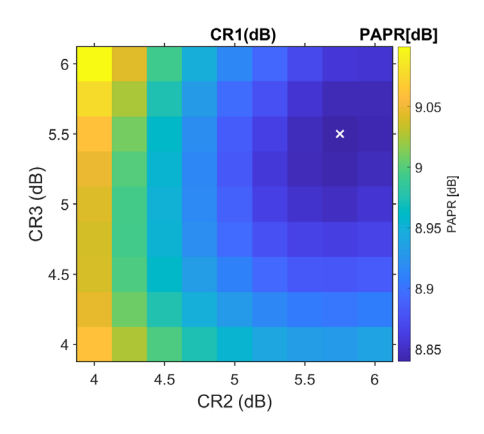


Fig. 8: The achievable PAPR for adaptive CR values. The optimal PAPR value is marked with a white cross. Minimum PAPR = 8.7940 dB with optimal CR values of [4.50, 5.5, 5.75] dB.

The proposed scheme performs clipping with ACE for three iterations using the optimized CR values resulting from Fig. 8 followed by a single enlipping operation combined with ACE, which leads to further improvements in PAPR reduction, BER performance, and power gain. In Fig. 10, the PAPR CCDF shows a notable PAPR reduction of the processed signal curve compared to the original signal. This enhancement is achieved through iterative clipping combined with ACE, effectively reducing the signal's high peaks.

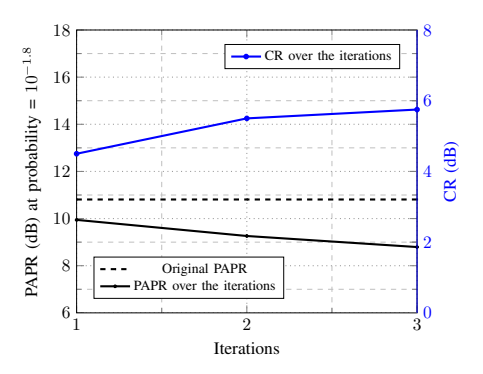


Fig. 9: PAPR and CR values vs clipping iterations for different numbers of subcarriers.

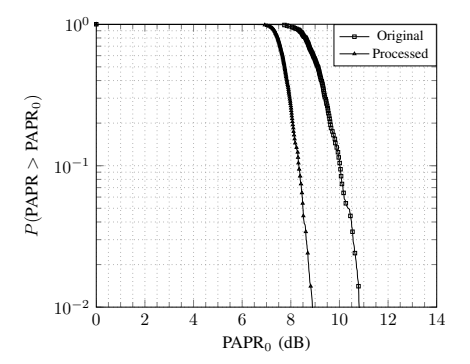


Fig. 10: CCDF of PAPR.

In addition, in Fig. 11a, the BER performance in function of the SNR is shown, and it can be seen that the proposed method produces a gain of 1 dB. This enhancement is due to the enlipping stage, which amplifies the average signal power, consequently improving the BER performance. Furthermore, Fig. 11b shows The PSD of the original and processed signals. The processed signal displayed negligible spectral regrowth, meeting the necessary out-of-band emission limit, and the spectral mask of the FBMC signal was kept.

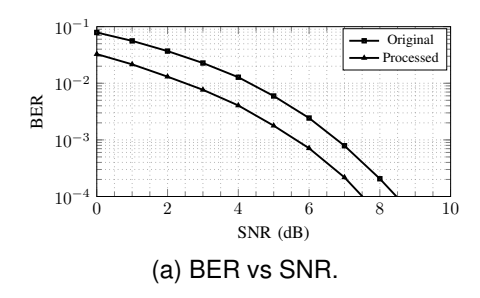
Fig. 12 illustrates the increase in power obtained through the iterative approach. The gain stays low throughout the initial three iterations of clipping and ACE, but a significant increase can be observed after implementing the last step, achieving 3.91 dB power gain. This highlights the technique's capacity to preserve signal integrity while boosting power.

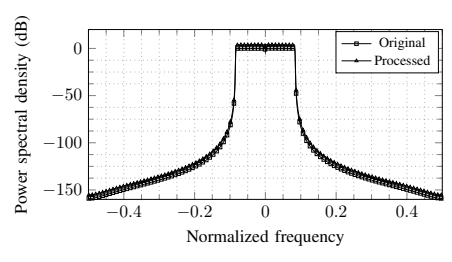
The efficacy of the PAPR reduction method is assessed through a gain metric  $(\Theta)$ , which considers both PAPR reduction and the extra signal power utilized. Following the formulation in [11], the definition of PAPR gain is as follows:

$$\Theta = \max_{m} \{ PAPR(x[m])_{dB} \} - \max_{m} \{ PAPR(x_{new}[m])_{dB} \} + \Delta P_s,$$
(8)

where

- $\max_{m} \{ PAPR(x[m])_{dB} \}$ : The maximum PAPR of the original signal.
- $\max_m \{ \text{PAPR}(x_{\text{new}}[m])_{\text{dB}} \}$ : The maximum PAPR of the processed signal.
- $\Delta P_s = 10 \cdot \log_{10} \left( \frac{\text{Power of processed signal}}{\text{Power of the original signal}} \right)$





(b) Power Spectral Density (PSD).

Fig. 11: Statistical analysis of the proposed scheme.

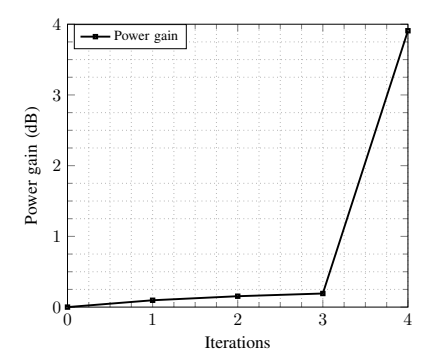


Fig. 12: Power gain.

After 3 iterations of clipping and ACE, a PAPR reduction gain of 2.24 dB is achieved, combining the power gain with the PAPR gain results in an overall gain metric of 6.15 dB. The proposed method achieves a higher  $\Theta$  than the iterative clipping and ACE method in [11] as we can see in Fig. 13, requiring fewer iterations to reach superior performance. Although the traditional approach consistently enhances  $\Theta$  with an increasing number of iterations, the additional step in the proposed method dramatically elevates  $\Theta$ , minimizing the requirement for further iterations and enhancing efficiency in complexity. This renders the proposed method more robust and computationally efficient for PAPR reduction.

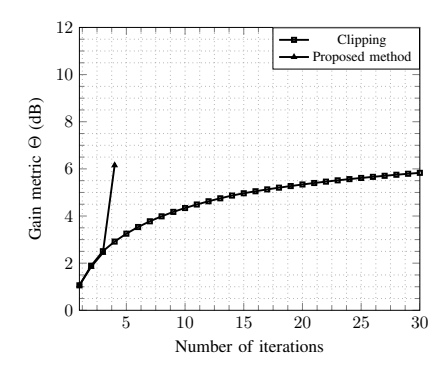


Fig. 13: Gain metric.

# TABLE II NOTATION USED IN COMPLEXITY ANALYSIS

| Symbol   | Description   |
|--|---|
| $M_{ m mod}$ $M_{ m demod}$ $M_{ m total}$ $I$ $N$ $K$ | Number of multiplications in one FBMC modulation<br>Number of multiplications in one FBMC demodulation<br>Total number of multiplications of the proposed scheme<br>Number of iterations<br>Number of subcarriers<br>Overlapping factor |

### V. ANALYSIS OF THE COMPUTATIONAL COMPLEXITY OF THE ITERATIVE PAPR REDUCTION SCHEME

In this section, the computational complexity of the proposed approach is derived; the analysis focuses explicitly on the number of multiplications required in the FBMC modulator and demodulator, as other steps introduce negligible overhead. The proposed method depicted in Fig. 6 include the following signal processing steps:

- 1) Initial modulation, generating the original FBMC signal.
- 2) Iteration steps consisting of clipping, demodulation, ACE, and modulation operations.
- 3) A final step for enlipping, demodulation, ACE, and modulation operations to generate the FBMC signal with reduced PAPR and enlarged signal power.

The main symbols used in the complexity analysis are summarized in Table II. Using this notation, the total number of multiplications required can be expressed as follows:

$$M_{\text{total}} = M_{\text{mod}} + I \cdot (M_{\text{demod}} + M_{\text{mod}}) + M_{\text{demod}} + M_{\text{mod}},$$
(9)

where the required number of multiplications of the modulator and demodulator can be expressed based on [19] for PPN using a single IFFT/FFT based on the number of subcarriers N, the overlapping factor K, and the number of iterations I as

$$M_{\text{mod}} = N(\log_2 N - 3) + 4 + 4KN, \tag{10}$$

$$M_{\text{demod}} = N(\log_2 N - 3) + 4 + 4KN.$$
 (11)

As a result, the number of multiplications required for the proposed scheme in the function of the iterations can be given based on (9), (10), and (11) as

$$M_{\text{total}} = (2I + 3)(N(\log_2 N - 3) + 4 + 4KN). \tag{12}$$

| COMPANSON OF THE REDUCTION METHODS.   |                      |                      |            |                |  |  |
|---------------------------------------|----------------------|----------------------|------------|----------------|--|--|
| Method                                | Side information     | Bit-rate loss        | Complexity | Power increase |  |  |
| PTS (Partial Transmit Sequences) [20] | Yes (phase index)    | Yes (SI bits)        | High       | No             |  |  |
| SLM (Selected Mapping) [20]           | Yes (sequence index) | Yes (SI bits)        | High       | No             |  |  |
| TI (Tone Injection) [21]              | No                   | No                   | High       | Yes            |  |  |
| TR (Tone Reservation) [10]            | No                   | Yes (reserved tones) | Low        | Yes            |  |  |
| Clipping (+ ACE) [22]                 | No                   | No                   | Low        | No             |  |  |
| Proposed Method                       | No                   | No                   | Low        | Ves            |  |  |

TABLE III COMPARISON OF PAPR-PEDUCTION METHODS

The required number of multiplications based on (12) for 3 iterations is shown Fig. 14. The plot depicts the overall computational complexity of the suggested approach in the function of the number of subcarriers. The figure also reveals the number of multiplications required in the case of the standard FS- and PPN-based approaches. The analysis shows a linear growth in complexity with a growing number of subcarriers. The results indicate that the FS and PPN approaches exhibit significantly higher computational complexity than the suggested PPN approach.

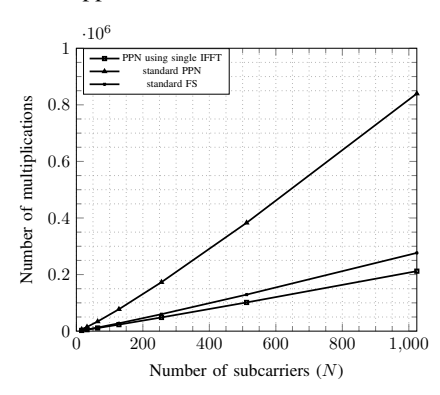


Fig. 14: Required number of multiplications of the iterative PAPR reduction method with 3 iterations using FS, PPN, and PPN with single IFFT as modulator and demodulator.

To provide a structured view of common PAPR-reduction techniques, Table III summarizes qualitative trade-offs for side information, bit-rate loss, complexity, and power increase for the proposed method and representative baselines.

## VI. CONCLUSIONS

In this paper, a statistical analysis of FBMC signals was conducted, including evaluating the CCDF of PAPR and kurtosis for different numbers of subcarriers. A novel method for minimizing PAPR in FBMC systems was presented. The proposed scheme applies three iterations of (clipping and ACE) to suppress the most significant peaks, followed by one iteration of (enlipping and ACE) to increase average signal power and improve BER performance. The CR values were optimized for each iteration by searching a range to determine the CR schedule that minimizes the resulting PAPR. The introduced enlipping aids improve the BER performance by raising the average signal power. The proposed scheme performed better in PAPR reduction and BER performance than the conventional schemes while maintaining computational efficiency.

#### ACKNOWLEDGMENTS

This study receives partial funding from the National Research Development and Innovation Office (NKFIH) via the OTKA Grant (K 142845) and the János Bolyai Research Grant (BO/00042/23/6) provided by the Hungarian Academy of Sciences.

#### REFERENCES

- [1] Z. Kollár and H. Al-Amaireh, "FBMC transmitters with reduced complexity," Radioengineering, vol. 27, no. 4, pp. 1147-1154, 2018, **DOI**: 10.13164/re.2018.1147.
- [2] M. Rahim, T. Stitz, and M. Renfors, "Analysis of clipping-based PAPR-reduction in multicarrier systems," in VTC Spring 2009-IEEE 69th Vehicular Technology Conference. IEEE, 2009, pp. 1–5, DOI: 10.1109/VETECS.2009.5073391.
- [3] E. Costa, M. Midrio, and S. Pupolin, "Impact of amplifier nonlinearities on OFDM transmission system performance," IEEE Communications Letters, vol. 3, no. 2, pp. 37–39, 1999, **DOI**: 10.1109/4234.749355.
- [4] B. Horváth and P. Horvath, "Establishing lower bounds on the peak-to-average-power ratio in filter bank multicarrier systems," in Infocommunication Journal, 2015.
- [5] P. Mishra and M. Amin, "PAPR reduction in OFDM using various coding techniques," International Journal of Wireless and Mobile Computing, vol. 15, no. 1, pp. 16-20, 2018, DOI: 10.1504/IJWMC.2018.10015847.
- [6] N. Shi and S. Wei, "A partial transmit sequences based approach for the reduction of peak-to-average power ratio in FBMC system," in 2016 25th Wireless and Optical Communication Conference (WOCC). IEEE, 2016, pp. 1–3, **DOI**: 10.1109/WOCC.2016.7506550.
- [7] S. Ramavath and U. C. Samal, "Theoretical analysis of PAPR companding techniques for FBMC systems," Wireless Personal Communications, vol. 118, no. 4, pp. 2965-2981, 2021, DOI: 10.1007/s11277-021-08164-1.
- C. Yang, R. Liu, L. Zhao, and Y. Wei, "Modified SLM scheme of FBMC signal in satellite communications," *IET Communications*, vol. 13, no. 11, pp. 1702–1708, 2019, **DOI**: 10.1049/iet-com.2018.5101.
- [9] R. Gopal and S. K. Patra, "Combining tone injection and companding techniques for PAPR reduction of FBMC-OQAM system," in 2015 Global Conference on Communication Technologies (GCCT). IEEE, 2015, pp. 709–713, **DOI**: 10.1109/GCCT.2015.7342756.
- [10] M. Laabidi, R. Zayani, and R. Bouallegue, "A new tone reservation scheme for PAPR reduction in FBMC/OQAM systems," in 2015 International Wireless Communications and Mobile Computing Conference (IWCMC). IEEE, 2015, pp. 862-867, DOI: 10.1109/IWCMC.2015.7289196.
- [11] Z. Kollár, L. Varga, B. Horváth, P. Bakki, and J. Bitó, "Evaluation of clipping based iterative PAPR reduction techniques for FBMC systems," The Scientific World Journal, vol. 2014, no. 1, p. 841 680, 2014, **DOI**: 10.1155/2014/841680.
- [12] B. Tahir, S. Schwarz, and M. Rupp, "Ber comparison between convolutional, turbo, ldpc, and polar codes," in 2017 24th International Conference on Telecommunications (ICT), 2017, pp. 1–7, DOI: 10.1109/ICT.2017.7998249.

- [13] Z. Tagelsir, H. Al-Amaireh, and Z. Kollár, "Active constellation extension with enlipping technique for PAPR reduction in FBMC-OQAM systems," in 2024 34th International Conference Radioelektronika (RADIOELEKTRONIKA), 2024, pp. 1–5, DOI: 10.1109/RADIOELEKTRONIKA61599.2024.10524051.
- [14] M. Bellanger, D. Le Ruyet, D. Roviras, M. Terré, J. Nossek, L. Baltar, Q. Bai, D. Waldhauser, M. Renfors, T. Ihalainen *et al.*, "FBMC physical layer: a primer," *Phydyas, January*, vol. 25, no. 4, pp. 7–10, 2010, technical report. [Online]. Available: http://www.ict-phydyas.org
- [15] L. Varga and Z. Kollár, "Low complexity FBMC transceiver for FPGA implementation," in 2013 23rd International Conference Radioelektronika (RADIOELEKTRONIKA). IEEE, 2013, pp. 219–223, poi: 10.1109/RadioElek.2013.6530920.
- [16] H. Al-Amaireh, "Optimization of FBMC-OQAM transceiver architectures," Ph.D. dissertation, Budapest University of Technology and Economics, Budapest, Hungary, 2021. [Online]. Available: https://repozitorium.omikk.bme.hu/items/ee124ef3-fabb-4ceb-8a4ea5ecc9aebc96
- [17] B. Krongold and D. L. Jones, "PAR reduction in OFDM via active constellation extension," *IEEE Transactions on broadcasting*, vol. 49, no. 3, pp. 258–268, 2003, **DOI**: 10.1109/ICASSP.2003.1202695.
- [18] B. Horvath and B. Botlik, "Optimization of tone reservation-based PAPR reduction for ofdm systems," *Radioengineering*, vol. 26, no. 3, pp. 791–797, 2017, **DOI**: 10.13164/re.2017.0791.
- [19] H. Al-Amaireh and Z. Kollár, "Complexity comparison of filter bank multicarrier transmitter schemes," in 2018 11th international symposium on communication systems, networks & digital signal processing (CSNDSP). IEEE, 2018, pp. 1–4, DOI: 10.1109/CSNDSP.2018.8471795.
- [20] T. Jiang and Y. Wu, "An overview: Peak-to-average power ratioreduction techniques for OFDM signals," *IEEE Transactions on broadcasting*, vol. 54, no. 2, pp. 257–268, 2008, DOI: 10.1109/TBC.2008.915770.
- [21] M. C. P. Paredes and M. Garcia, "The problem of peak-to-average power ratio in OFDM systems," arXiv preprint arXiv:1503.08271, 2015, DOI: 10.48550/arXiv.1503.08271.
- [22] Y.-C. Wang and Z.-Q. Luo, "Optimized iterative clipping and filtering for PAPR reduction of OFDM signals," *IEEE Transactions on communications*, vol. 59, no. 1, pp. 33–37, 2010, DOI: 10.1109/TCOMM.2010.102910.090040.



Zahraa Tagelsir received her MSc degree in Electrical Engineering in 2018 from the University of Khartoum. She started her PhD studies in 2022 at the Budapest University of Technology and Economics (BME). Her research interests include digital signal processing and wireless communication.



**Zsolt Kollár** is an Associate Professor in the Department of Artificial Intelligence and Systems Engineering at the Budapest University of Technology and Economics (BME). His research focuses on wireless communication systems, signal processing, and cognitive radio technologies.